Shock Hugoniot of osmium up to 800 GPa from first principles calculations

2009 J. Phys.: Condens. Matter 21 415402

(http://iopscience.iop.org/0953-8984/21/41/415402)

J. Phys.: Condens. Matter **21** (2009) 415402 (6pp) doi:10.1088/0953-8984/21/41/415402

Shock Hugoniot of osmium up to 800 GPa from first principles calculations

K D Joshi, Satish C Gupta and S Banerjee

Bhabha Atomic Research Centre, Mumbai 400085, India

E-mail: kdj@barc.gov.in

Received 22 June 2009, in final form 11 August 2009
Published 23 September 2009
Online at stacks.iop.org/JPhysCM/21/415402

Abstract

First principles total energy calculations on hcp, ω (a three atom simple hexagonal), β (bcc) and fcc phases of osmium have been performed as a function of hydrostatic compression employing the FP-LAPW method. The comparison of total energies of these phases up to a maximum compression $V/V_0 = 0.58$ (pressure $\sim$ 700 GPa) shows that the hcp structure remains stable up to this compression. The 300 K isotherm is determined after adding finite temperature thermal contributions to the total energy calculated as a function of volume at 0 K. From the theoretically determined isotherm, we have derived the shock Hugoniot of this metal and determined the shock parameters C_0 and s to be 4.48 km s^{-1} and 1.32, respectively. Employing the theoretically calculated Gruneisen parameter in the differential form of the Lindemann melting rule, we have determined the variation of melting point of the osmium with pressure. The theoretically derived melting curve and the temperature rise along the Hugoniot predict the shock melting of osmium at $\sim$447 GPa with a corresponding temperature of $\sim$9203 K.

1. Introduction

Osmium metal, located in the middle of the 5d series, adopts a hexagonal closed packed structure and has the highest density among elements under ambient temperature and pressure conditions. This metal is very difficult to machine as it is extremely hard and brittle. Moreover, it is difficult to handle since it forms a toxic oxide when its powder is exposed to air. Because of these difficulties, the experimental work on this material under high pressure has been very limited. For example, no report is available for studies on osmium in shock wave experiments, which require the preparation of large sized samples of well defined shapes. However, recently, high pressure experiments using a diamond anvil cell (DAC), which require very small samples of a few tens of micron in dimensions have been reported [1–4].

The first experimental high pressure work on this metal was reported by Cynn *et al* [1]. Based on the measurement of the high pressure equation of state (EOS) of this metal up to 65 GPa using energy dispersive x-ray diffraction in the DAC and determination of the zero pressure bulk modulus (B_0), the authors claimed that the bulk modulus of osmium (462 GPa) is higher than that of diamond (445 GPa). This study was immediately followed by the theoretical analysis by Joshi *et al* [5], who reanalysed the experimental data of Cynn *et al*, and also carried out first principle calculations and found that the bulk modulus of Os is comparable with, but not more than, that of diamond. Since then there have been many experimental and theoretical high pressure studies on this material. A high pressure powder x-ray diffraction study up to 58 GPa at room temperature by Kenichi [2] with a better hydrostatic condition in the DAC reported the B_0 of Os to be 395 $\pm$ 15 GPa, which is lower than that of diamond. This study revealed that the c/a ratio of Os increases monotonically from 1.5800 at an ambient pressure condition to 1.5856 at 58 GPa. Similarly, Voronin *et al* [3] studied the high pressure–high temperature behaviour of this metal up to 15 GPa and 1273 K using energy dispersive x-ray diffraction in a T-cup 6–8 high pressure apparatus. This apparatus is basically a two stage multi-anvil system, with a first stage consisting of a steel cylinder split into six parts enclosing a cubic cavity of dimension $\sim$20 mm and the second stage which consists of an assembly of eight cubes of polycrystalline diamond or WC having an edge length of 10 mm. Further, these cubes are separated by spacers and one corner of each cube is truncated into a triangular face, the eight truncations form an octahedral cavity in which the sample with the pressure transmitting medium is compressed [6]. In yet another angle dispersive x-ray diffraction study under static high pressure carried out using the DAC, Occelli *et al* [4] determined the 300 K isotherm of Os up to 75 GPa. This

study suggested an iso-structural phase transition in Os near 25 GPa manifested by the anomaly in the rate of change of c/a ratio with pressure. All these experimental studies are limited to a pressure up to 75 GPa. Higher pressure measurements under hydrostatic conditions are difficult as the compressibility of the gasket materials (including rhenium) is higher than that of Os. Due to higher compressibility of the gasket material and the pressure transmitting medium than that of the osmium sample, there is a possibility of the Os sample coming into contact with the anvils of the DAC leading to the destruction of hydrostaticity in the pressure. Thus, for generating the high pressure equation of state data one has to resort to the use of first principles methods.

In the present study, we have carried out *ab initio* theoretical calculations on Os up to a few Mbar pressures. We have examined the stability of its crystal structure, determined the 300 K isotherm and the generated shock Hugoniot. Further, we have studied the variation of melting temperature with pressure and determined the melting temperature under shock compression.

2. Theoretical method

In order to analyse the structural stability under hydrostatic compression, the calculation of total energy as a function of volume has been performed on hcp, ω (three atom simple hexagonal cell), β (bcc) and fcc phases of osmium employing a density functional approach based full potential linearized augmented plane wave (FP-LAPW) method (WIEN 97 package [7]) within the generalized gradient approximation (GGA) for the exchange–correlation energy. The muffin tin radius used for all the structures is 1.8 au. The parameter $RK_{\max}$ that determines the number of basis functions (size of matrices) is chosen to be 10. Here R is the muffin tin radius and $K_{\max}$ is the magnitude of the largest K vector (reciprocal lattice vector) used in the plane wave expansion. The dimension of $K^2_{\max}$ is that of energy i.e. Rydberg. Before doing the calculations a k-point convergence test was carried out at the volume corresponding to the experimental equilibrium volume. For this we varied the number of k-points in the Brillouin zone from 500 to 9000. We found the k-point convergence at approximately 8000 k points. Hence, for further calculations we used 8000 k-points in the full Brillouin zone. In order to examine the behaviour of the c/a ratio with compression for the hcp structure, at each volume, we have carried out the total energy calculations as a function of c/a, and determined the optimum value of this ratio that corresponds to the lowest total energy. This process is repeated for several volumes and optimized c/a values were determined. The ω-phase, which is an AlB_2-type structure is treated as having two inequivalent sites with one atom at site (0, 0, 0) ('Al' site) and one atom each at sites (2/3, 1/3, 1/2) and (1/3, 2/3, 1/2) ('B' site) [8, 9]. The c/a ratio for the ω phase is taken to be the ideal value of 0.61. The calculations have been performed up to a volume compression of ∼0.58. The structural stability analysis is carried out by comparing the total energy of the hcp, ω, β and fcc phases under hydrostatic compression. The 300 K isotherm, Hugoniot and pressure effect on melting of osmium are determined as follows.

2.1. Isotherm at 300 K

In order to generate the theoretical isotherm a polynomial fit between the total energy versus unit cell volume is carried out and the pressure as a function of volume at 0 K from this fit is determined using the following expression:

$$P = -\frac{\partial E_c}{\partial V}, \tag{1}$$

where E_c is the total energy and V is unit cell volume. The zero pressure bulk modulus (B_0) and its pressure derivative at zero pressure (B_0') were obtained by fitting the P–V data to the third order Birch Murnaghan equation of state:

$$P = \tfrac{3}{2}B_0(\eta^{-7/3} - \eta^{-5/3})[1 + \tfrac{3}{4}(B_0' - 4)(\eta^{-2/3} - 1)], \tag{2}$$

where $\eta = V/V_0$. Here V and V_0 are the volume at a given pressure and volume at zero pressure, respectively. The bulk modulus B and its pressure derivative B' at various volumes are then determined from equation (2) as follows:

$$B = -V\frac{\partial P}{\partial V} \qquad \text{and} \qquad B' = \frac{\partial B}{\partial P} = -\frac{V}{B}\frac{\partial B}{\partial V}. \tag{3}$$

To determine the 300 K isotherm we have adopted the following procedure. The total energy and pressure at given temperature T and volume V can be expressed as [10–13]

$$E(V,T) = E_c(V) + E_T(V,T) + E_e(V,T) \tag{4}$$

$$P(V,T) = -\frac{\partial F(V,T)}{\partial V} = -\frac{\partial F_c}{\partial V} - \frac{\partial F_T(V,T)}{\partial V} - \frac{\partial F_e(V,T)}{\partial V}, \tag{5}$$

where $F(V,T)$ is the Helmholtz free energy at temperature T and volume V with F_c, denoting the free energy at 0 K, and $F_T(V,T)$ and $F_e(V,T)$ corresponding to the thermal lattice and thermal electronic contributions, respectively. Equation (5) can equivalently be written as [10, 11, 14]

$$P(V,T) = -\frac{\partial E_c(V)}{\partial V} + \frac{\gamma E_T}{V} + \gamma_e\frac{E_e}{V}. \tag{6}$$

Here E_T is the thermal lattice contribution including the zero point vibration energy and $E_e = \frac{1}{2}\beta T^2$ is thermal electronic contribution to the total energy. γ and γ_e are the vibrational and electronic Gruneisen parameters, respectively. β is the coefficient of electronic specific heat. At 300 K the electronic contributions are very small, hence to determine the 300 K isotherm these terms in equations (4) and (6) are neglected. γ is determined using the following definition:

$$\gamma = -\frac{\partial \ln \theta_D}{\partial \ln V}. \tag{7}$$

Here, θ_D is the pressure dependent Debye temperature, which is determined using the following expression [11, 13]:

$$\theta_D = 251.45\sqrt{\frac{M}{\rho}}V_M^{-\frac{1}{3}}, \tag{8}$$

where the mean modulus M, density ρ and molar volume V_M are in GPa, g cm^{-3} and cm^3 mol^{-1}, respectively. M is defined as (derived in the appendix)

$$M = 3^{\frac{5}{3}}\left(\frac{B}{(1+\sigma)}\right)\left[\left(\frac{1}{1-\sigma}\right)^{\frac{3}{2}} + 2\left(\frac{2}{1-2\sigma}\right)^{\frac{3}{2}}\right]^{-\frac{2}{3}}. \quad (9)$$

The Poisson ratio (σ) required for determination of M is taken to be 0.25 from the literature (www.webelements.com). The E_T per atom including zero point energy is determined using the high temperature limit of the Debye model of lattice vibrations [11, 15]:

$$E_T = 3k_BT\left[1 + \left(\frac{1}{20}\right)\left(\frac{\theta_D}{T}\right)^2 - \left(\frac{1}{1680}\right)\left(\frac{\theta_D}{T}\right)^4\right]. \quad (10)$$

Here k_B is the Boltzmann constant.

Finally the 300 K isotherm is evaluated by substituting the value of γ and E_T calculated at $T = 300$ K using equations (7) through (10) in equation (6).

2.2. Shock Hugoniot

The shock Hugoniot of osmium is determined by applying the procedure followed by Gupta *et al* [13]. For this purpose we used equations (4) and (6) in the Rankine–Hugoniot equation according to which the increase in total energy of a material upon shock compression from an initial volume of V_0 to a final volume of V is expressed as [16, 17]

$$E(V, T_H) - E(V_0, T_0) = \tfrac{1}{2}[P(V, T_H) + P(V_0, T_0)] \times [V_0 - V]. \quad (11)$$

Here T_H is the temperature rise along the shock Hugoniot and T_0 is the room temperature.

At the high temperatures generated during shock compression i.e. $T \gg \theta_D$ the expression for E_T is reduced as

$$E_T = 3k_BT. \quad (12)$$

As the temperatures generated during shock compressions are high it is also essential to consider the contribution of electronic excitations. The β and γ_e required for evaluation of electronic contributions to energy and pressure are determined using the following expressions [11, 18]:

$$\beta = \pi^2 k_B^2 N(E_f)/3, \quad (13)$$

where $N(E_f)$ is the density of states at the Fermi level, which is determined at various unit cell volumes from FP-LAPW calculations, and

$$\gamma_e = \frac{\partial \ln \beta}{\partial \ln V}. \quad (14)$$

Finally, using the energies $E(V, T)$ and corresponding pressures $P(V, T)$ calculated according to equations (4) and (6) the Hugoniot was determined by finding the temperature and pressure for which the Rankine–Hugoniot relation is satisfied at each volume.

2.3. The pressure effect on melting and shock induced melting

The pressure effect on melting is determined using the procedure followed by Soma *et al* [19]. In the Debye model, the root mean square displacement $\langle u^2\rangle$ at a temperature T higher than Debye temperature θ_D is expressed as [18]

$$\langle u^2\rangle = \frac{3\hbar^2 T}{mk_B\theta_D^2}, \quad (15)$$

where m is the atomic mass. Lindemann's law for melting states that at the temperature, at which the ratio of the square root of the mean square displacement to the nearest neighbour distance exceeds a limit x_{melt}, melting of a solid starts. Mathematically it is expressed as follows.

For melting to occur the

$$\frac{\sqrt{\langle u^2\rangle}}{R_1} \geqslant x_{melt}, \quad (16)$$

where R_1 is the nearest neighbour distance. Using equations (15) and (16) the melting temperature can be expressed as

$$T_{melt} = \frac{x_{melt}^2}{3\hbar^2} mk_B\theta_D^2 R_1^2. \quad (17)$$

This equation in differential form can be written as [19]

$$\frac{d(\ln T_{melt})}{d(\ln V)} = -2\gamma + \frac{2}{3}. \quad (18)$$

This differential equation, solved by satisfying the melting point T_{melt} ($\eta = 1$) under atmospheric pressure with crystal volume V_0, yields [19]

$$T_{melt}(y) = T_{melt}(1)\exp\left[2\int_\eta^1 \frac{\gamma(\eta) - 1/3}{\eta} d\eta\right]. \quad (19)$$

The variation in melting temperature as a function of compression η is determined using the theoretically determined $\gamma(\eta)$ in equation (19). The melting temperature is plotted as a function of compression or corresponding pressure. Finally, the temperature rise along the Hugoniot and the melting temperature as a function of pressure are plotted together and the crossover of the two curves yields the shock pressure and corresponding temperature at which melting of Os occurs under shock compression.

3. Results and discussions

To analyse the structural stability of the osmium, the total energy calculated for the hcp, ω, β and fcc phases under hydrostatic compression is plotted against the unit cell volume in figure 1, which displays the total energy of these phases relative to the hcp structure. This figure shows that the hcp structure is lowest in energy, hence it is thermodynamically a stable structure up to the maximum compression $\eta = 0.58$ (~700 GPa). The 0 K isotherm determined from the polynomial fit of total energy with volume gives the value of V_0 to be 14.41 (Å)^3/atom as compared to the experimental value of 13.97 (Å)^3/atom [4]. The B_0 and B_0'

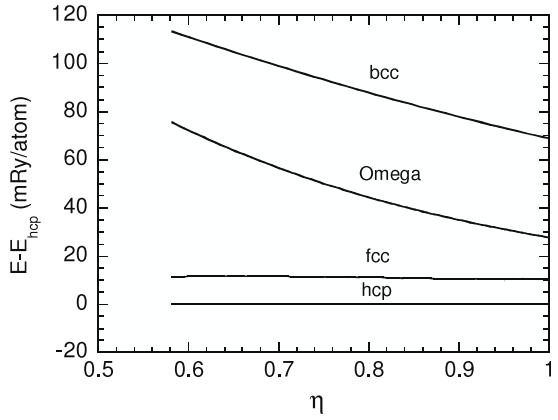

Figure 1. Total energy as a function of hydrostatic compression for various phases of osmium. Total energies for various phases are plotted relative to the hcp phase.

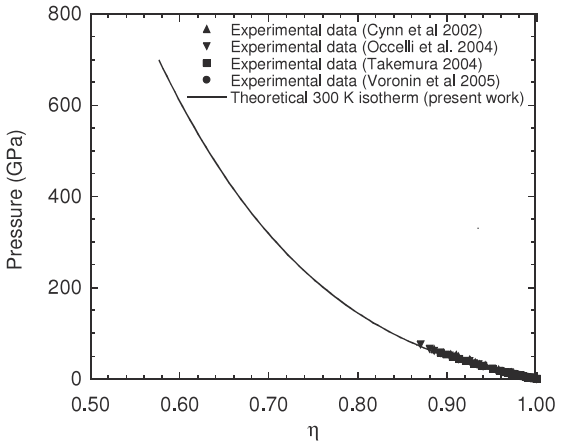

Figure 2. 300 K isotherm of osmium.

obtained by fitting the 0 K isotherm to the third order Birch Murnaghan EOS are 442 GPa and 3.96, as compared to the experimental values ranging from 395 to 462 GPa and 4.5–2.4, respectively [1–4]. The 300 K isotherm obtained after adding the thermal contributions at 300 K to the theoretically determined 0 K isotherm is displayed in figure 2. For a better comparison with experimental data the 300 K isotherm for lower compressions is plotted in figure 3. The theoretical 300 K isotherm agrees well with the experimental data. For determination of the 300 K isotherm from the 0 K isotherm, we have calculated the volume dependent Debye temperature, the value of which at ambient volume is obtained as being 474 K as compared to the experimental value of 500 K [18].

Figure 4 displays the theoretically determined optimum c/a at 0 K along with experimental data [1–4] as a function of pressure. Our calculations show that the c/a ratio increases with increasing pressure monotonically and does not show any anomalous behaviour.

The Hugoniot determined from the theoretical isotherm is plotted in the P–η plane in figure 5. The same is represented in figure 6 as a relation between the shock velocity (U_s) and particle velocity (U_p) by using the two shock jump conditions, namely the mass and momentum conservation equation [17]. Figure 6 shows that the Hugoniot in the U_s–U_p plane is linear

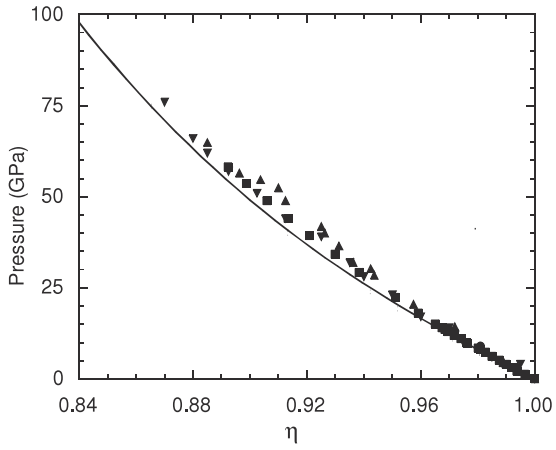

Figure 3. 300 K isotherm for osmium for small compressions.

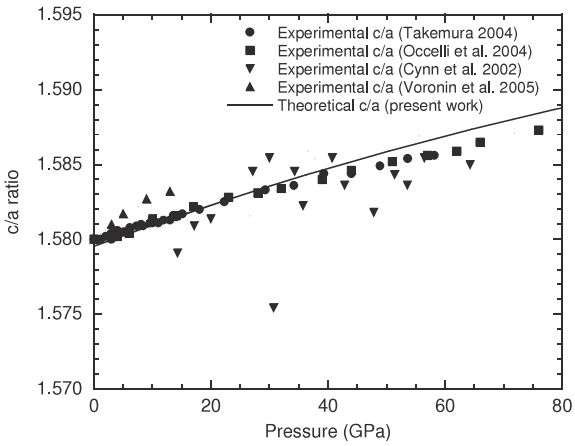

Figure 4. Optimized c/a ratio as a function of pressure for osmium.

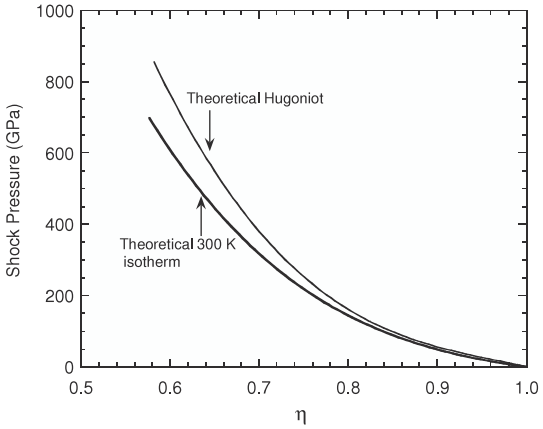

Figure 5. Hugoniot of osmium represented in the P–η plane. The theoretical 300 K isotherm is also shown.

($U_s = C_0 + sU_p$). The U_s–U_p behaviour is fitted to a straight line, where C_0 corresponds to the bulk sound speed. The values of C_0 and s evaluated from the linear fit between the theoretically determined U_s and U_p are 4.48 km s^{-1} and 1.32, respectively.

The pressure dependence of the melting temperature is determined using equation (19). As shown in figure 7, for

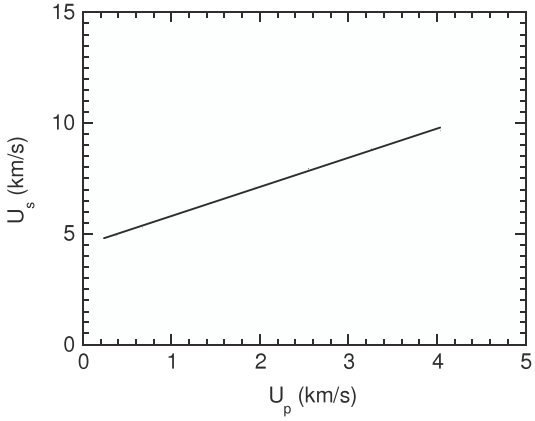

Figure 6. Shock velocity as a function of particle velocity in osmium.

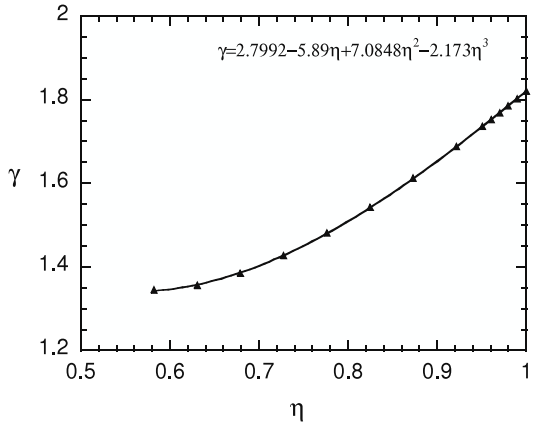

Figure 7. γ as a function of η for osmium. The symbols show γ calculated theoretically at various η and the solid curve shows a polynomial fit of γ with η.

this purpose γ determined as a function of volume from equation (7) is fitted to η and a functional relationship between γ and η (displayed in figure 6) is obtained. The room pressure melting temperature $T_{\rm melt}$ (1) used in equation (19) is taken as 3306 K from the literature [18]. Figure 8 displays the melting temperature as a function of pressure for this metal. Also, the temperature rise calculated along shock Hugoniot is plotted in this figure. It is clear from figure 7 that the Hugoniot crosses the melting curve at a pressure of ∼447 GPa and temperature of ∼9203 K, suggesting that shock induced melting in osmium will start at this pressure.

4. Summary

The structural stability analysis of Os shows that the hcp phase is energetically favourable over the ω, β and fcc phases up to a compression of ∼0.58 (corresponding pressure ∼ 700 GPa). The quantities V_0, B_0, B_0' and $\theta_{\rm D}$ determined theoretically agree well with the experimental values. The 300 K isotherm derived from the 0 K isotherm shows excellent agreement with the experimental data. The Hugoniot of Os is predicted from the theoretically determined 0 K isotherm. From the linear

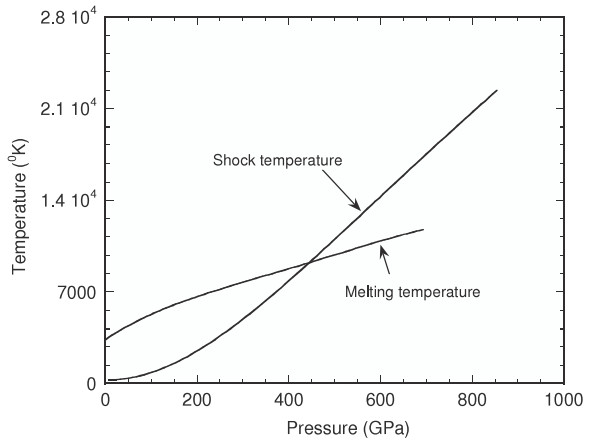

Figure 8. The melting temperature and shock temperature as a function of pressure for Os.

fit of the theoretically determined $U_{\rm s}$–$U_{\rm p}$ values the C_0 and s are determined to be 4.48 km s^{-1} and 1.32, respectively. Using the Lindemann law of melting in conjunction with our theoretically determined volume dependent Gruneisen parameter, we have determined the pressure effect on melting. From the theoretically determined temperature rise along the Hugoniot and the pressure dependence of melting, we have predicted the shock melting of Os to occur at ∼447 GPa with a corresponding temperature of 9203 K.

Appendix

The expression for M is derived using the following approach. In the Debye model of lattice vibrations the Debye temperature ($\theta_{\rm D}$) and cut-off frequency ($\omega_{\rm D}$) are related as follows [18]:

$$\theta_{\rm D} = \frac{\hbar\omega_{\rm D}}{k_{\rm B}}. \tag{A.1}$$

In Debye model the velocity of sound for each type of polarization is taken to be constant i.e. the solid is considered as a classical elastic continuum. Under this approximation the cut-off frequency and cut-off wavevector ($K_{\rm D}$) are related as

$$\omega_{\rm D} = CK_{\rm D}, \tag{A.2}$$

where C is the average velocity of sound. $K_{\rm D}$ is given as [18]

$$K_{\rm D} = \left(\frac{6\pi^2 N}{V}\right)^{\frac{1}{3}}. \tag{A.3}$$

Here N is number of primitive cells and V is the corresponding volume. Substituting equations (A.2) and (A.3) into equation (A.1) one gets

$$\theta_{\rm D} = \frac{\hbar}{k_{\rm B}}\left(\frac{6\pi^2 N}{V}\right)^{\frac{1}{3}} C. \tag{A.4}$$

If we take V as the molar volume ($V_{\rm M}$) then N becomes the Avogadro number. Then substituting the values of the constants in equation (A.4) in CGS units we get

$$\theta_{\rm D} = 2.5145 \times 10^{-3} V_{\rm M}^{-\frac{1}{3}} C. \tag{A.5}$$

In the Debye model for an isotropic solid the average sound velocity is the weighted mean of the velocities for one longitudinal and two degenerated transverse polarizations:

$$\frac{1}{C^3} = \frac{1}{3}\left(\frac{1}{C_{\mathrm{L}}^3} + \frac{2}{C_{\mathrm{T}}^3}\right), \tag{A.6}$$

where C_{L} and C_{T} are the velocities for the longitudinal and transverse polarizations, respectively. C_{L} and C_{T} are related to the elastic moduli as follows:

$$C_{\mathrm{L}} = \sqrt{\frac{B + \frac{4}{3}G}{\rho}} \qquad \text{and} \qquad C_{\mathrm{T}} = \sqrt{\frac{G}{\rho}}. \tag{A.7}$$

Here B, G and ρ are the bulk modulus, shear modulus and density, respectively. For an isotropic solid the Poisson ratio (σ) and elastic moduli are related as follows:

$$\sigma = \frac{3B - 2G}{2(3B + G)}. \tag{A.8}$$

The above equation can also be expressed in the following forms:

$$B + \tfrac{4}{3}G = \tfrac{2}{3}(1-\sigma)(3B+G);$$
$$G = \tfrac{1}{3}(1-2\sigma)(3B+G); \qquad 3B + G = \frac{9}{2}\frac{B}{(1+\sigma)}. \tag{A.9}$$

Using equations (A.9) the C_{L} and C_{T} can be rewritten as

$$C_{\mathrm{L}} = \sqrt{\frac{3B(1-\sigma)}{\rho(1+\sigma)}} \qquad \text{and} \qquad C_{\mathrm{T}} = \sqrt{\frac{3B(1-2\sigma)}{2\rho(1+\sigma)}}. \tag{A.10}$$

Substitution of C_{L} and C_{T} from equations (A.10) to equation (A.6) yields

$$\frac{1}{C} = \frac{1}{3^{\frac{1}{3}}}\left(\frac{3B}{\rho(1+\sigma)}\right)^{-\frac{1}{2}}\left[\left(\frac{1}{1-\sigma}\right)^{\frac{3}{2}} + 2\left(\frac{2}{1-2\sigma}\right)^{\frac{3}{2}}\right]^{\frac{1}{3}}$$

or

$$C = 3^{\frac{1}{3}}\left(\frac{3B}{\rho(1+\sigma)}\right)^{\frac{1}{2}}\left[\left(\frac{1}{1-\sigma}\right)^{\frac{3}{2}} + 2\left(\frac{2}{1-2\sigma}\right)^{\frac{3}{2}}\right]^{-\frac{1}{3}}$$

or $\quad C = \sqrt{\dfrac{M}{\rho}}, \quad$ with

$$M = 3^{\frac{5}{3}}\left(\frac{B}{(1+\sigma)}\right)\left[\left(\frac{1}{1-\sigma}\right)^{\frac{3}{2}} + 2\left(\frac{2}{1-2\sigma}\right)^{\frac{3}{2}}\right]^{-\frac{2}{3}}. \tag{A.11}$$

References

[1] Cynn H, Klepeis J E, Yoo C-S and Young D A 2002 *Phys. Rev. Lett.* **88** 135701
[2] Kenichi T 2004 *Phys. Rev.* B **70** 012101
[3] Voronin A, Pantea C, Zerda T W, Wang L and Zhao Y 2005 *J. Phys. Chem. Solids* **66** 706
[4] Occelli F, Farber D L, Badro J, Aracne C M, Teter D M, Hanfland M, Canny B and Couzinet B 2004 *Phys. Rev. Lett.* **93** 095502
[5] Joshi K D, Jyoti G and Gupta Satish C 2003 *High Pressure Res.* **23** 403
[6] Parise J B, Weidner D J, Chen J, Libermann R C and Chen G 1998 *Annu. Rev. Mater. Sci.* **28** 349
[7] Blaha P, Schwarz K, Sorantin P and Trickey S B 1990 *Comput. Phys. Commun.* **59** 399
[8] Sikka S K, Vohra Y K and Chidambaram R 1982 *Prog. Mater. Sci.* **27** 245
[9] Joshi K D, Jyoti G, Gupta Satish C and Sikka S K 2002 *Phys. Rev.* B **65** 0521061
[10] Gospodinov V 1999 arXiv:cond-mat/99114072-v2 [cond-mat.mtrl-sci]
[11] Godwal B K and Jeanloz R 1989 *Phys. Rev.* B **40** 7501
[12] Zel'dovich Ya B and Raizer Yu P 1967 *Physics of Shock Waves and High Temperature Hydrodynamic Phenomena* vol 2 (New York: Academic)
[13] Gupta S C, Joshi K D and Banerjee S 2008 *Metall. Mater. Trans.* A **39** 1593
[14] Wallace D C 1998 *Phys. Rev.* B **58** 15433
[15] Wallace D C 1972 *Thermodynamics of Crystals* (New York: Wiley)
[16] Band W and Duvall G E 1961 *Am. J. Phys.* **29** 780
[17] Duvall G E and Fowles G R 1963 *Shock Waves in High Pressure Physics and Chemistry* vol 2, ed R S Bradley (New York: Academic) p 209
[18] Kittel C 1995 *Introduction to Solid State Physics* (New York: Wiley)
[19] Soma T, Matsuo Kagaya H and Nishigaki M 1983 *Phys. Status Solidi* b **116** 673